Energy, Volume 191, January 2020, Article number 116562
DOI: 10.1016/j.energy.2019.116562

Characterization of solid char produced from pyrolysis of the organic fraction of municipal solid waste, high volatile coal and their blends

Diyar Tokmurzin[a], Botagoz Kuspangaliyeva[a,b], Berik Aimbetov[a], Bexultan Abylkhani[a], Vassilis Inglezakis[b,c], Edward J Anthony[d], Yerbol Sarbassov[a,b,c*]

[a]*Green Energy and Environment Laboratory, National Laboratory Astana, Nazarbayev University, Astana 010000, Kazakhstan;*
[b]*Environmental Science & Technology Group, Chemical & Materials Engineering Department, School of Engineering, Nazarbayev University, Astana, 010000, Kazakhstan;*
[c]*Environment & Resource Efficiency Cluster (EREC), Nazarbayev University, Astana, 010000, Kazakhstan;*
[d]*Combustion and CCS Centre, Cranfield University, Cranfield MK43 0AL, United Kingdom;*
*Corresponding authors: +7(7172) 605752; E-mail address: ysarbassov@nu.edu.kz

(*Yerbol Sarbassov*)

Abstract

In this study, the organic fraction of municipal solid waste (Org-MSW) was blended with high-volatile coal (HVC) in proportions of 25/75%, 50/50%, 75/25% by weight. Pyrolysis of these mixtures was then investigated in a thermogravimetric analyzer (TGA) and a horizontal tube furnace under a nitrogen environment. The mass loss rate of samples, differential thermogravimetry (DTG) curves and kinetic analysis of the samples were compared for both blended and non-blended samples. Higher gas yields were seen with increasing pyrolysis temperature for both samples. In addition, the kinetic analysis indicated that the apparent activation energy values of org-MSW samples varied from 535 to 5284 kJ/kmol (over the temperature range of 100 to 887°C), while the values for HVC were 247 to 962 kJ/kmol. The activation energy for HVC varied with temperature and the highest value of 2036 kJ/kmol was found in the temperature range of 336-490°C. Comparable results were obtained between the TGA and fixed bed tests on the residual char fraction. The findings of

this work will be very important in developing a co-firing technology for solid waste residuals and coal for energy production.

Keywords: Pyrolysis, organic waste, high volatile coal, char characterization

Abbreviation

DTG	differential thermogravimetry
GCV	gross calorific value
HDPE	high-density polyethylene
HVC	high-volatile coal
ID	internal diameter
LDPE	low-density polyethylene
LVC	low-volatile coal
MSW	municipal solid waste
Org-MSW	organic fraction of municipal solid waste
PET	polyethylene terephthalate
PP	polypropylene
TGA	thermogravimetric analysis
WtE	waste to energy
XRD	X-ray diffraction

Nomenclature

a	conversion rate
A	pre-exponential factor (1/s)
Ea	activation energy (kJ/kmol)
$f(a)$	kinetic model reaction
H	heating rate (°C/min)
M	weight of sample (mg)
m_f	final weight of sample (mg)
m_o	initial weight of sample (mg)
m_t	weight at time t (mg)

R	gas constant (8.314 J/mol/K)
T	temperature (K)
T	time (min)
T_f	final temperature (K)
T_i	Initial temperature (K)
P	atmospheric pressure (bar)

1. Introduction

According to the World Bank, MSW generation including organic waste is expected to increase to 2.2 Gt (1.42 kg per person per day) by 2025 [1-2]. In 2012, 1.3 Gt of municipal solid waste (MSW) was generated worldwide (1.2 kg per person per day), mainly in urban areas [1]. In addition, it has been noted that low-income countries have the highest fraction of organic waste of around 62% in the total waste stream [1]. Growth of income in developing countries inevitably leads to an increase of MSW generation per capita and waste generation is expected to outpace the population growth by more than double by 2050 [3]. The European strategy on solid waste management imposes the following waste minimization hierarchy: prevention, reuse, recycling, other recovery methods such as energy recovery and disposal [4]. Thus, energy recovery is an attractive option to be used for those waste streams where materials recovery is not effectively used [5]. However, more efficient and sustainable waste-to-energy (WtE) technologies are more suited to megacities where large amounts of MSW are available [6]. Considering that the average heating value of MSW is around 10 MJ/kg [7], the application of waste to energy is broader than incineration, and can be associated with electricity and district heating production [8-9].

The pyrolysis process is an alternative thermochemical method to convert various solid waste materials into value-added solid fuel products [10]. Along with syngas produced as by-product, the pyrolysis of such wastes allows one to produce different types of chemical products or fuels [11]. In addition, the energy obtained from the pyrolysis processes is associated with reduced carbon dioxide, nitrogen oxides and sulfur dioxide emissions, in contrast to emissions produced by WtE plants [12-13]. These lower emissions are mainly achieved due to the inert

environment [12]. In addition, high-quality solid fuel products can be obtained from the pyrolysis processes [14].

Thermogravimetric analysis and fixed bed pyrolysis tests are reliable methods of obtaining preliminary results of fuel properties and knowledge on conversion temperatures during thermal treatment. To date, the kinetics of the pyrolysis of mixed solid waste [15], plastics [16], tires, biomass, refuse-derived fuels (RDF) and various coals have been studied by means of thermogravimetric analysis (TGA) [17]. Co-pyrolysis (pyrolysis of mixed wastes and coal) of biomass/coal blends [18-19], coal/plastic mixtures [20-21] and biomass/MSW [22] have also been investigated in TGA and fixed bed reactors. Table 1 provides a list of studies that investigated co-pyrolysis of coal and various waste materials such as paper, plastic, biomass and others. Overall, it appears that co-pyrolysis is an optimal method for valorization of various wastes to syngas, chemicals production, and residual solid fuel production. In addition, chars produced from pyrolysis of polyethylene (PET) resulted in improved coke properties [23].

Table 1. Studies on co-pyrolysis of coal and various waste materials

Type of reactor & pyrolysis	**Fuel samples**	**Heating rate, (°C/min)**	**Temp (°C)**	**Comments**	**Ref**
Slow pyrolysis in a fixed bed (quartz tube, D-60mm, L-500mm)	Coal with PET	5	900	The addition of PET to coal in coking blends had impacts on coke yield, mean volume and pore surface area	[23]
Fixed bed (quartz tube, D-95mm, L-500mm)	Coal with waste tires	5	900	The obtained tars contained mostly maltenes (80–85 wt%) with lower aromaticity	[24]
Fixed bed	Zhundong	10-40	600-	Improved porosity,	[25]

(quartz tube D-30mm) and TGA	lignite and pine sawdust		800	increased gas yield, ash catalytic effect	
TGA, Screw reactor (D-12cm, L-150cm)	High-sulfur coal, olive stone and wheat	10	900 TGA 873 reactor	Improved desulfurization, and solid fuel quality	[26]
TGA	Co-pyrolysis paper sludge and MSW blends	30-50	1000	Pyrolysis characteristics showed better values when coal proportions were less than half.	[27]
TGA	Rubber tires, plastic waste	30	900	Kinetic model was developed. The rate constant of some reactions showed non-linear temperature dependence on the logarithmic form of Arrhenius law	[28]
TGA	Low-volatile coal/plastics (HDPE, LDPE, PP)	20	900	Coal is decomposed at lower temperatures, temperature range of organic matter de-volatilization region is found to be broader	[21]

Even though org-MSW is primarily sourced from biomass with high volatile content, there are only limited studies on its co-pyrolysis blended with high-volatile coal [21][23-28]. This study investigates the thermal properties of blended and non-blended org-MSW and HVC samples by pyrolysis in the TGA and horizontal fixed bed tube furnace. Preliminary tests of org-MSW and high-volatile coal blend pyrolysis have been conducted in a fixed bed reactor by Tokmurzin et al. [29]. In an extension of this study, representative low and high temperatures of 500°C and 800°C were selected for fixed bed pyrolysis tests to compare thermal decomposition behavior of samples. Additionally, the mass balance of org-MSW and HVC pyrolysis products was provided from fixed bed pyrolysis tests. Further,

characterizations of org-MSW and HVC char were conducted to provide thermal properties and elemental analysis, and solid char atomic structure was explored with X-ray diffraction (XRD) to investigate the crystalline structures of the samples. Based on the obtained data, pyrolysis of residual org-MSW and HVC, and their blends were discussed.

2. Materials and methods

2.1. Sample preparation

The organic fraction of MSW (org-MSW) was collected from the sampling campaign of the municipal solid waste produced in Astana city. A more detailed description of the MSW sampling procedure can be found elsewhere [29]. In this study, org-MSW samples consist of multiple components such as food waste, fruit waste and fine waste fractions. High-volatile coal (HVC) samples were obtained from the Shubarkol coal deposit in the northern region of Kazakhstan. The received org-MSW samples were shredded first with a garden shredder to a size reduction of 10-15 mm, followed by shredding in a rotary cutting mill to achieve a final sample size of around 1 mm. Org-MSW and HVC samples were well mixed and quartered for further analysis. Samples were sieved and dried at 105°C for 24 h in a dryer.

2.2. Properties of org-MSW and HVC samples

Table 2 presents the proximate and ultimate analyses of tested Org-MSW and HVC feedstocks. The initially received org-MSW and HVC samples were prepared and subjected to a proximate analysis in accordance with ASTM D3172 – 13 (Standard Practice for Proximate Analysis of Coal and Coke) and ASTM E870-82 (2019) Standard Test Methods for Analysis of Wood Fuels which were performed in a muffle furnace, (Carbolite Gero ELF), while ultimate analyses were obtained from

an elemental analyzer (vario MICRO cube Elementar, Germany) in accordance with ASTM D5373 – 16 Standard Test Methods for Determination of Carbon, Hydrogen and Nitrogen in Analysis Samples of Coal and Carbon in Analysis Samples of Coal and Coke [30-31-32-33-34-35]. The calorific values were measured by a bomb calorimeter (B-08MA Etalon, Kazakhstan) using a sample weight between 0.5-1 g in oxygen gas at a pressure of 30 bar (see Table 2).

Table 2. Proximate and ultimate analysis of HVC and Org-MSW

Samples23	Org-MSW	HVC	25%/75% (Org-MSW/HVC)	50%/50% (Org-MSW/ HVC)	75%/25% (Org-MSW/ HVC)
Proximate, (wt% as received)					
Moisture	3.40	5.96	5.33	4.53	3.91
Volatile matter	59.35	40.30	45.09	49.95	54.70
*Fixed carbon**	23.35	51.30	44.27	37.39	30.46
Ash	13.90	2.44	5.31	8.14	10.94
Ultimate (wt.%, dry ash free)					
Carbon	46.16	69.72	63.83	57.9	52.05
Hydrogen	6.23	6.05	6.1	6.1	6.19
Nitrogen	4.18	1.71	2.33	2.95	3.56
Sulfur	0.26	1.05	0.85	0.66	0.46
*Oxygen**	43.17	21.47	26.9	32.32	37.75
GCV, MJ/kg	17.77	26.97	24.67	22.37	20.07

*O by difference;

2.3. Experimental setup

A horizontal tube furnace was used for pyrolysis and co-pyrolysis tests of org-MSW and HVC samples. The tube furnace is shown in Fig. 1. The furnace consists of a gas cylinder, gas flow meter, tubular furnace, quartz tube, gas analyzer and

impingers for tar collection. The exit area of the quartz tube was heated with a tape heater and kept at a temperature of 350°C to avoid tar condensation in the quartz tube. The exit gas passed through a series of impingers filled with an isopropanol solution (99.7%). Prior to the experiments, the temperature profile along the length of the quartz tube was measured by K-type thermocouples. The flow rate of 0.186 m^3/h (at STP conditions) was set as an optimal flow rate to maintain the residence time of gas at around 3-5 s over the heated zone of the quartz tube furnace. In addition, the temperature was measured in the middle of the quartz tube and this was taken as the mean temperature.

For a typical test, a dry solid sample was introduced into the ceramic tube (internal diameter (ID) of 25 mm and a length of 20 mm) and placed in the center of the quartz tube. Sample weights were about 20 g (±0.1). The open space between the ceramic and quartz tube was then filled with quartz wool to ensure the flow of gas passes through the solid fuel sample. The ID of quartz tube was 54 mm, with a length of 1000 mm. Nitrogen (99.7%) was used as the inlet gas with a flow rate of 0.186 m^3/h (at STP conditions). The heating rate of the furnace was set to 20°C/min. A calibrated flowmeter (Dywer) was used to control the volumetric rate of the gas. The initial and remaining masses of solids were determined by a high-accuracy weighing scale. The tube furnace was held at the selected temperature for 30 min to ensure complete pyrolysis of samples. The complete pyrolysis process was monitored by gas analyzer (Rapidox 5100B, Cambridge Sensotec, UK). The remaining char samples were collected for further analysis.

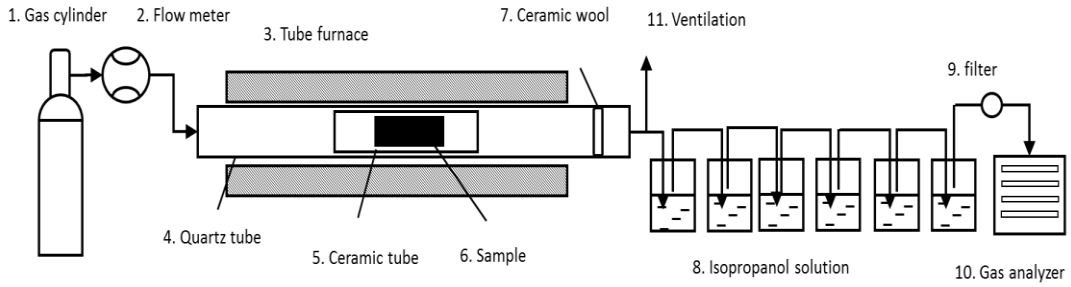

Fig. 1. Experimental sketch of the fixed bed reactor

2.4. Experimental procedure

Fig. 2 shows the experimental procedure performed for pyrolysis of org-MSW and HVC samples, and these are described in greater detail below. Initially, prepared samples of Org-MSW and HVC as described in section 2.1 were pyrolyzed under an inert environment in the horizontal tube furnace as discussed in section 2.3. Experimental conditions for the fixed bed pyrolysis tests are shown in Table 3.

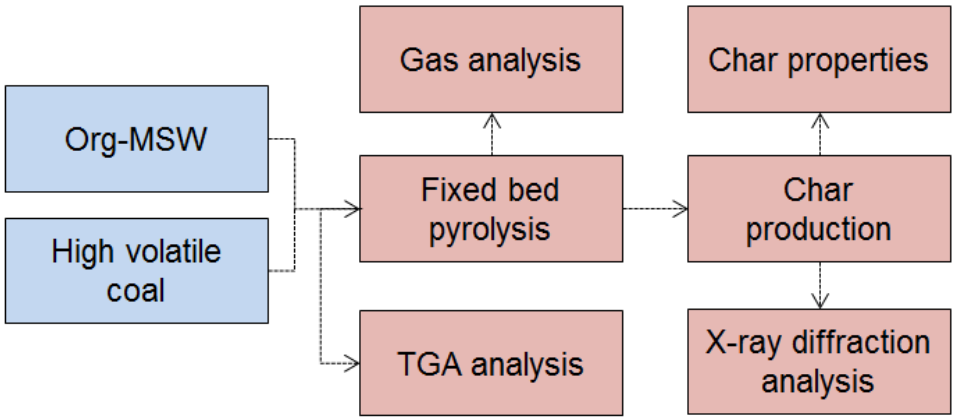

Fig. 2. Schematic procedure of org-MSW and HVC pyrolysis

Pyrolysis of samples was performed at atmospheric pressure. In addition, tests were done at 500°C and 800°C under constant heating rate and a N_2 environment.

Table 3. Experimental conditions for pyrolysis tests

Test parameters	Lower value	Higher value
Operating temperature, °C	500	800
Gas environment	Nitrogen	Nitrogen
Flow rate, m^3/h	0.252	0.186
Total pyrolysis time, min	30	30
Heating rate, °C/min	20	20

In addition, the same samples were also tested in a TGA (TGA-STA 6000, Perkin Elmer). TGA tests were done in a N_2 environment to provide the weight loss curves and kinetic data for the initial solid samples. Small quantities of samples (20-30 mg) were heated at the rate of 20°C/min to 900°C with a 20-min hold time at the end. The inert gas was supplied at a flow rate of 0.0012 m^3/h with purity of 99.95%. Further, the residual char material was characterized by property analysis and X-ray diffraction (XRD model SmartLab, Rigaku, Japan). Proximate and ultimate analyses of char samples were performed according to ASTM D3172 – 13 [30] (see Table 3).

3. Results and discussion

3.1. Mass balance of pyrolysis products

The important parameters affecting MSW pyrolysis include temperature, heating rate, residence time of the gas over the heated zone and particle size of residual materials [12]. According to Chen et al. [12], the yield of the pyrolysis products char, liquid and gas is strongly governed by the pyrolysis temperature and residence time of the process. The typical gaseous products during pyrolysis consist of CO_2, CO, CH_4, H_2, C_2H_6 and C_3H_8 [12]. Table 4 presents the product mass balances for pyrolysis conducted at 500°C and 800°C with experimental conditions noted in

section 2.3. The solid char fraction of an org-MSW was 42% at the lower pyrolysis temperature, decreasing to 39% at 800°C. Similarly, the char fraction of HVC decreased from 73% at the lower temperature to 60.8% at the higher temperature. For tar products, an increase of the temperature in the reactor did not noticeably affect tar production for org-MSW and maintained levels of around 22-24%. The pyrolysis of an organic MSW, cellulose, had the highest yield of tar at 450-500°C, but slowly decreased at higher temperatures due to thermal cracking to non-condensable gases [36]. Similar results were also found during bench-scale pyrolysis of agricultural wastes, such as wheat straw, olive husks, grape residues, and rice husks, with maximum tar yield in the range from 500°C to 600°C [37]. Interestingly, agricultural wastes such as sugarcane bagasse and eucalyptus also gave similar devolatilization behavior, probably due to their lignocellulosic nature [38-39]. The increase of the temperature from 500°C to 800°C almost doubled the weight of tar produced for HVC samples. As expected, higher gas yields were observed at higher pyrolysis temperatures for both org-MSW and HVC samples. This could be explained by the stronger thermal cracking of samples and, thus, higher release of volatiles with temperature.

Table 4. Mass balance of products during pyrolysis of org-MSW and HVC

Sample	Temp, °C	Char, %	Tar, %			Gas yield*, %
			Heavy tar	Light tar	Total tar	
Org-MSW	500	42.1	18.5	6.3	24.8	33.1
	800	39.2	15.5	6.8	22.3	38.5
HVC	500	73.2	6.5	6.3	12.8	14.0
	800	61.8	9.4	14.3	23.7	14.5

*by difference

3.2. Thermogravimetric analysis of samples

The weight loss curves of HVC, org-MSW, and their blends during the TGA tests under a N_2 environment are shown in Fig. 3. Table 2 shows the proximate analysis of samples and indicates that the HVC sample had nearly 40.3% of volatiles, compared with 59.4% for an org-MSW. As seen in Fig. 3, the weight loss of HVC sample becomes almost 40% of its initial weight at 900°C, while the weight loss of an org-MSW is 80%. The remaining char content of HVC was consistent with weight loss curves produced under a N_2 environment, while a slightly greater weight loss curve was observed for org-MSW. This difference could be due to the further decomposition of char samples in the TGA. As anticipted, weight loss curves of org-MSW and HVC blends (25%/75%; 50%/50%, 75%/25%) agreed with the expected values for blends based on the org-MSW and HVC weight loss curves. Thus, an increase of org-MSW ratio in blended proportions with HVC increases overall conversion during the pyrolysis. Fig. 4 gives the DTG curves of the same samples. Three clear peaks can be seen from Fig. 4 for org-MSW, HVC and blended tests. DTG curves of samples showed the first peaks at 80-100°C, associated with the release of moisture content. The second and main peaks occur over the temperature range of 290-330°C for org-MSW and blended samples. Interestingly, the main decomposition temperatures were similar to those from a TGA study by Fang et al. [27] and Zhou et al. [40].

After reaching their maximum peaks, the DTG curves of org-MSW and blended samples decreased drastically when the temperature reached 400°C. Similar behavior was observed by Ferrara et al. [41] for a TGA study using blended wood

chips and South African coal. By contrast, HVC starts to react above 400°C and achieves its maximum peak in the range of 460-470°C. This curve was similar to South African coal as noted by Ferrara et al. [41]. DTG curves of blended org-MSW and HVC demonstrated onset temperatures for pyrolysis similar to pure org-MSW samples. At 300°C, the mass loss rates of blended samples were lowered according to the fraction of org-MSW. The third DTG peaks of the blended samples occurred in the temperature range of 460-470°C. Cai et al. [21] has investigated the pyrolysis of plastic wastes such as low-density polyethylene (LDPE), high-density polyethylene (HDPE), polypropylene (PP) and co-pyrolysis with a low-volatile coal (LVC) and observed the same sharp and narrow temperature ranges for the onset and end of pyrolysis. This can be explained by the presence of very similar molecular structures and bonds, which tend to break at a given temperature ranges. Coal, by contrast, demonstrated a wider pyrolysis range due to the heterogeneous nature of its structure [42]. Table 5 shows the pyrolysis characteristics of samples derived from TGA and DTG.

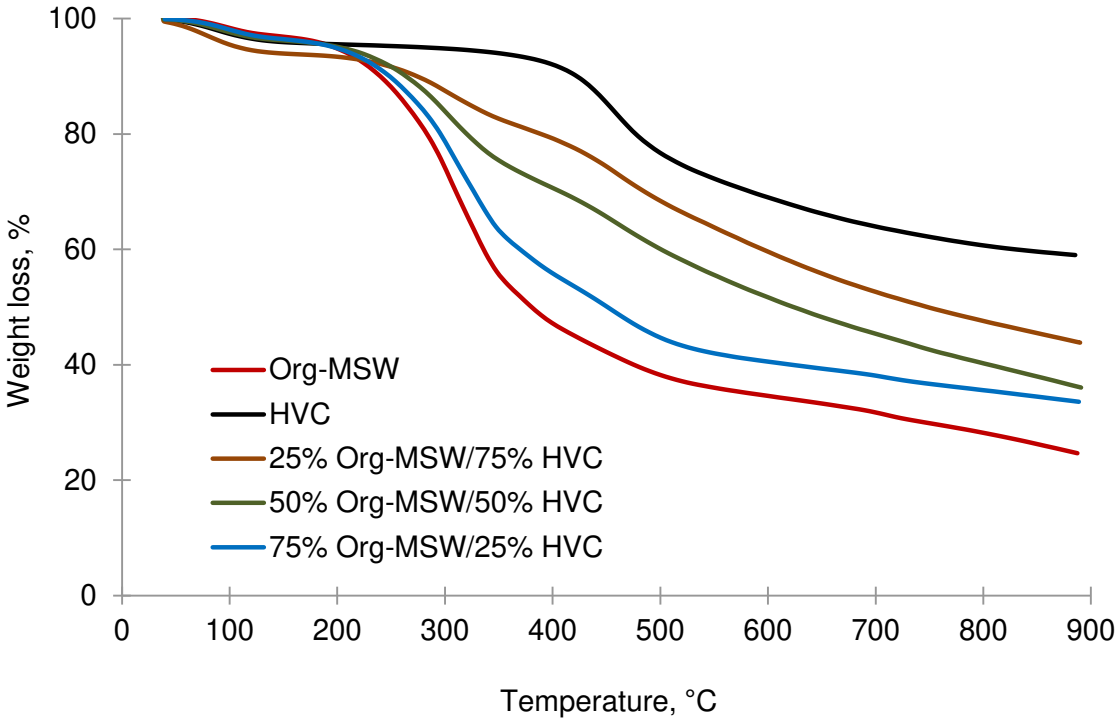

Fig. 3. Weight loss curves of HVC, org-MSW, and their blends during pyrolysis

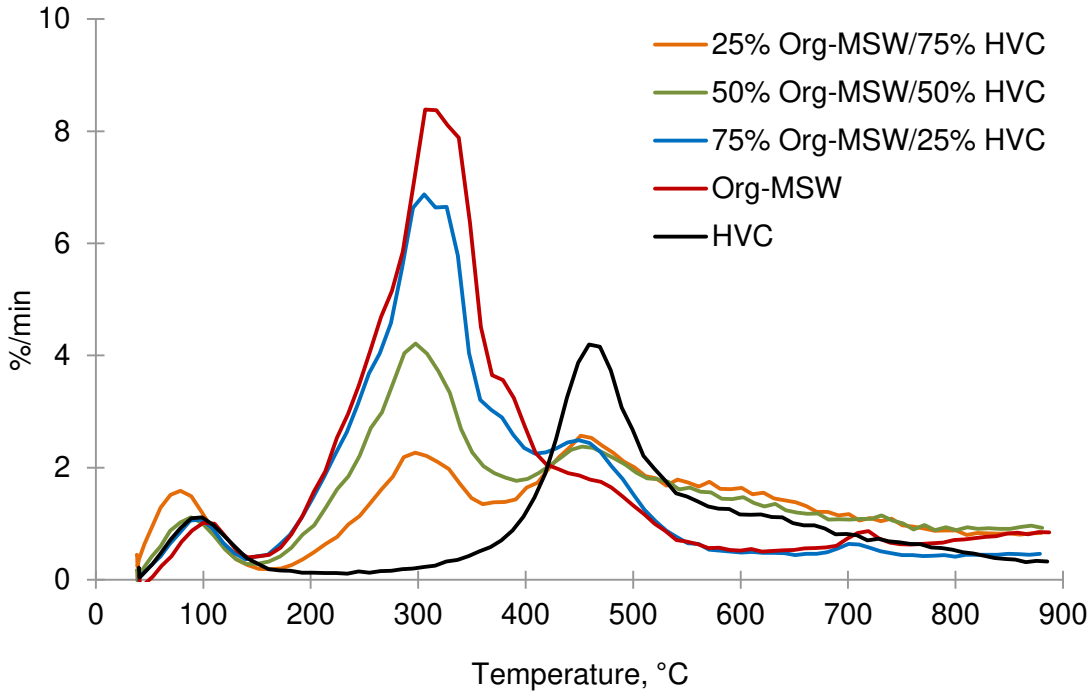

Fig. 4. DTG curves of HVC, org-MSW and their blends

Table 5. Pyrolysis characteristics of samples and weight loss rates at heating rate of 20 °C/min

Samples	Temperature range for max weight loss (°C)		$(dm_i/dt)_{max}$ (%/min^{-1})	Peak temperature (°C)	Residual weight
	T_I	T_F		T_P	(%)
HVC	360	880	4.2	459	59.0
Org-MSW	190	530	8.39	306	28.3
25%Org-MSW/75%HVC	170	870	2.57	461	47.6
50%Org-MSW/50%HVC	170	870	4.21	320	40.2
75%Org-MSW/25%HVC	170	870	6.87	316	35.6
HDPE [12-13]	477	521	56.0	505	15
LDPE [12-13]	438	509	43.9	493	8
PP [12-13]	447	503	46.0	491	5
LVC [12-13]	174	710	0.7	466	81

T_I-initial temperature; T_F- final temperature; T_p-peak temperature

In addition, the comparison of residual char was made between fixed bed and TGA tests for org-MSW and HVC samples. As can be seen from Table 4, the fixed bed pyrolysis tests at 800°C have an average char fractions of 39.2% for org-MSW and 61.8% for HVC. However, in TGA these values of char weights were 28.27% for org-MSW and 60.8% for HVC at 800°C. As can be seen, the weight of HVC samples has not changed significantly with increase of temperature. However, a

notable difference on char weight derived from org-MSW samples was observed. Due to the further increase of temperature in TGA from 800 to 900°C, the observed difference of residual char weights was 11%. This could be explained by further volatilization of org-MSW samples. Another possible factor could be the heterogeneity of samples. As highlighted above, the weight of samples used for fixed bed was around 20g and 0.02-0.03 g for TGA tests.

3.3. Kinetics of the org-MSW and HVC samples

The kinetic parameters, activation energy and pre-exponential factor, of HVC and org-MSW were determined by the integral method analysis assuming that solid fuel pyrolysis first-order [43-44]. The rate of solid phase reactions for heterogeneous org-MSW and HVC fuels can be expressed as equation (1) [42]:

$$\frac{d\alpha}{dt} = k(t)f(\alpha) = Aexp(-\frac{E}{RT})(1-a) \quad (1)$$

where da/dt is the rate of conversion, k is the rate constant, $f(a)$ is for reaction model, A is the pre-exponential Arrhenius factor (s^{-1}), E is the apparent activation energy (kJ/mol), R is the universal gas constant, and T is reaction temperature (K). The conversion rate (a) was defined from the following equation (2):

$$\alpha = \frac{m_o - m_t}{m_o - m_f} \quad (2)$$

where m_o is the initial weight of the sample (mg), m_t is the weight at time t, and m_f is final weight of the sample at the end of pyrolysis. For a constant heating rate, H, during pyrolysis, H=dT/dt; rearranging equation (1) and integrating gives [21],[44]:

$$ln\left[\frac{-ln(1-\alpha)}{T^2}\right] = ln\left[\frac{AR}{HE}\left(1-\frac{2RT}{E}\right)\right] - \frac{E}{RT} \quad (3)$$

It should be noted that for most values of E and for the temperature range of the pyrolysis, the expression $ln[AR/HE(1\text{-}2RT/E)]\text{-}E/RT$ on the right side of equation (3)

is constant. Thus, if the left side of Eq. (3) is plotted versus $1/T$, a straight line is obtained for a first-order reaction [44]. An activation energy E was determined from $-E/R$ slope, while pre-exponential factor was determined graphically.

Fig. 5 shows the plots of $\ln[-\ln(1-a)/T^2]$ versus 1/T for blended and non-blended samples. It can be clearly seen that the curves for HVC, org-MSW were not linear and indicated several stages at given temperatures. Here, following Cai et al. [21] and Melendi-Espina et al. [44], the pyrolysis of plastics was assumed to be a linear first-order process. Individual curves for $\ln[-\ln(1-a)/T^2]$ versus 1/T for org-MSW, HVC and their 50%/50% blends can be found in Fig. 6 (a-b-c). It can be seen that the $\ln[-\ln(1-a)/T^2]$ curves as a function of 1/T for each sample can be divided into several stages with 3-4 consecutive first-order reactions. In this regard, the HVC samples were divided into 3 stages, while org-MSW and blended samples were split into 4 stages. The conversion rate was recalculated for each stage separately. Fig. S.1 (a, b and c) (in Supplementary Materials) demonstrated linear pyrolysis stages. Activation energies for each stage were calculated from the slope of each plot along with the pre-exponential factor. Table 6 provides a summary of the activation energies, E, and pre-exponential factors, A, for each stage of HVC, org-MSW and their 50%/50% blends.

Table 6 Kinetic parameters for pyrolysis of HVC, Org-MSW, and their 50%/50% blend

Sample	Temp. (°C)	Conversion range (%)	E (kJ/mol)	A (min^{-1})	$-R^2$
HVC	100-336	97.4-94.3	246.7	$0.3x10^{-3}$	0.76
	336-490	94.3-78.1	2035.8	$4.7x10^{-20}$	0.99
	490-885	78.1-59.0	962.3	$3.8x10^{-3}$	0.93

Org-MSW	100-203	98.4-94.6	535.2	0.1	0.96
	203-369	94.6-52.1	1116.8	18.8	0.99
	369-778	52.1-28.9	635.9	$0.6x10^{-3}$	0.88
	778-887	28.9-24.7	5283.7	$67.1x10^{-9}$	0.97
50%Org-MSW/ 50% HVC	100-192	97.7-95.4	515.8	0.1	0.93
	192-319	95.4-80.3	1240.6	303.6	0.99
	319-781	80.3-41.1	581.9	$4.1x10^{-4}$	0.95
	781-890	41.1-36.1	5106.3	$17.2x10^{9}$	0.97

R^2 – correlation coefficient

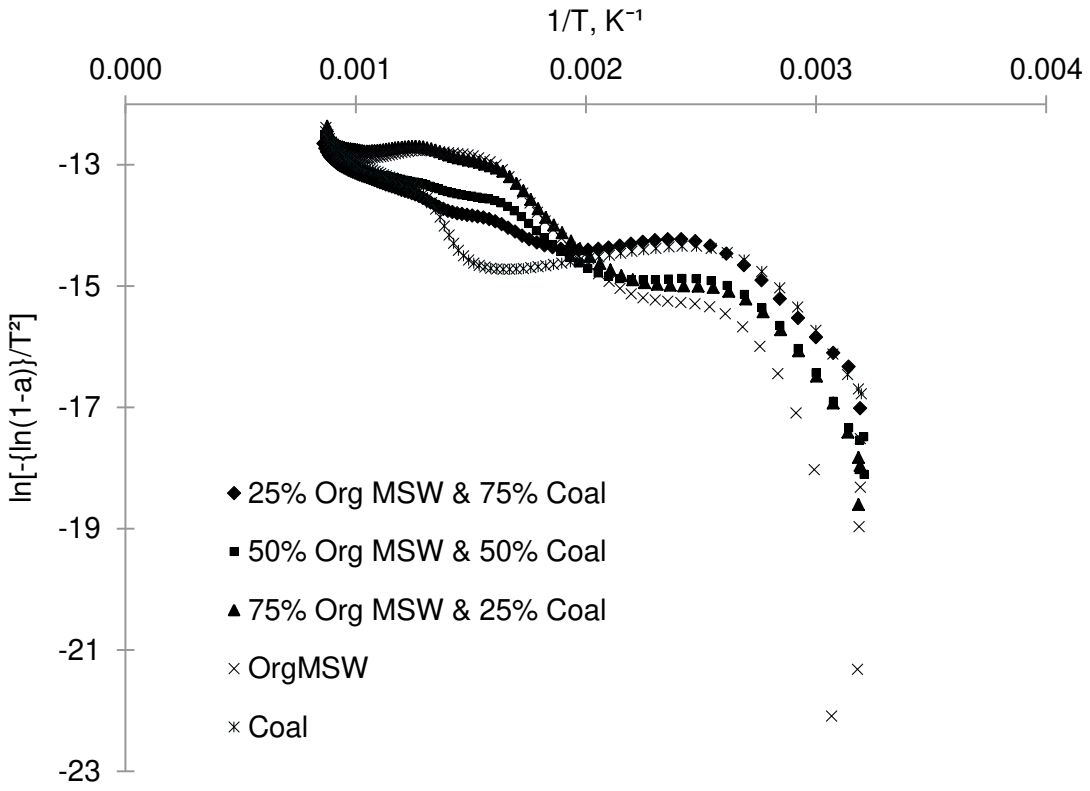

Fig. 5. Plots of ln[-ln(1-a)/T^2] vs 1/T for HVC, org-MSW and for blended tests

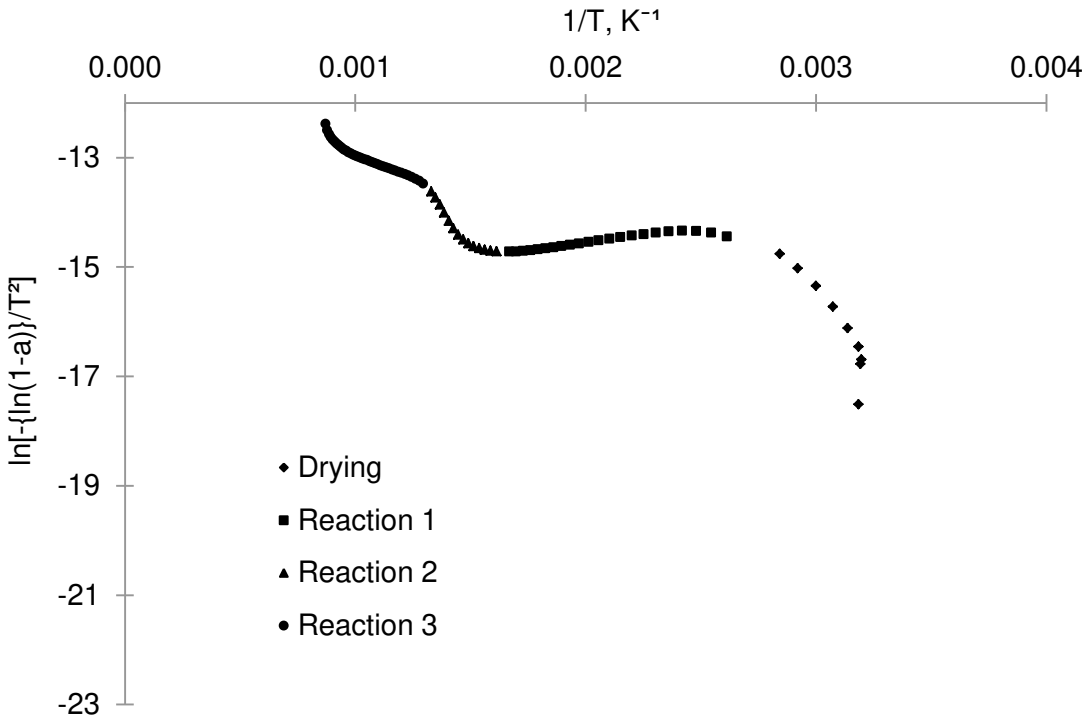

Fig. 6. (a) Plots of ln[-ln(1-a)/T^2] vs $1/T$ for HVC

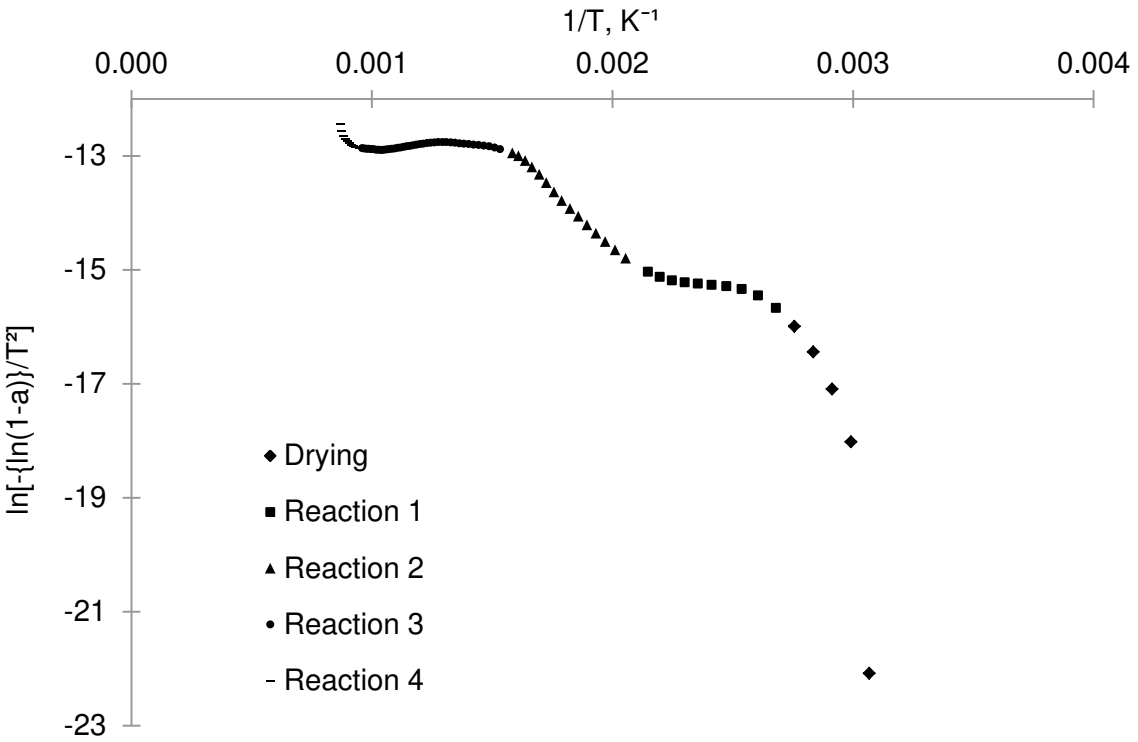

Fig. 6. (b) Plots of ln[-ln(1-a)/T^2] vs $1/T$ for org-MSW

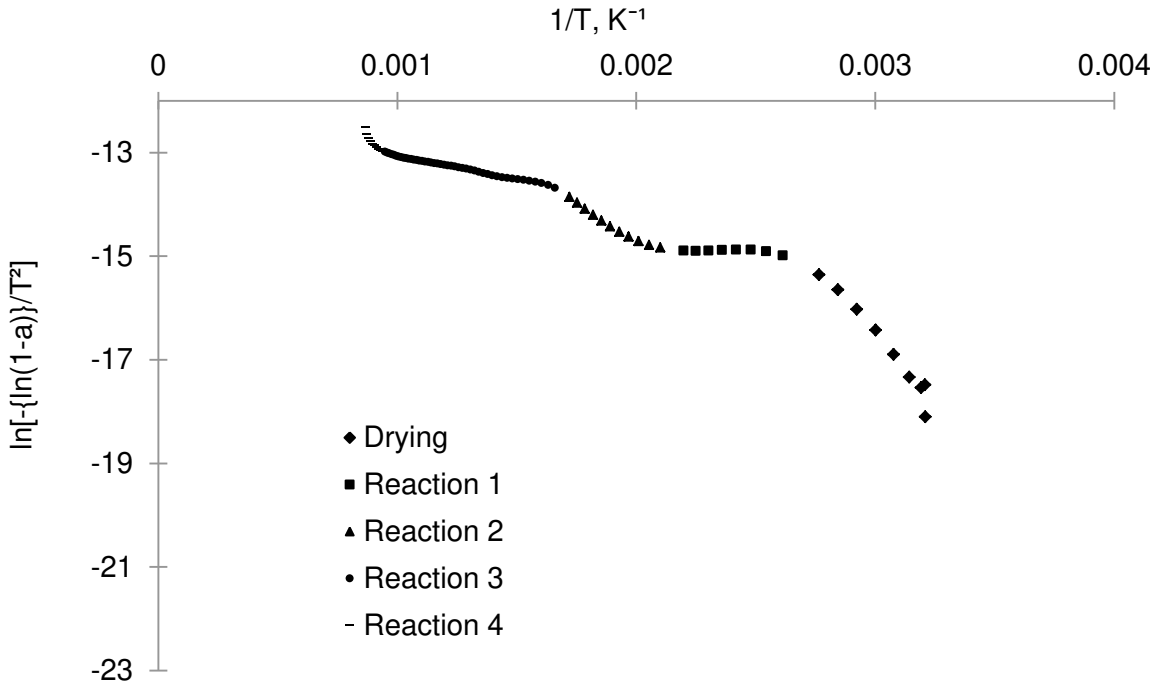

Fig. 6. (c) Plots of ln[-ln(1-a)/T^2] vs 1/T for 50%/50% blends

In the first stage for HVC samples, a slow conversion occurs between 100°C and 336°C with activation energy of 246 kJ/mol (see Table 6). This is followed by a

further increase of conversion rate at a temperature above 336°C and this region can be divided into two regions. First, a region between 336°C to 490°C and then a second one occurring in the temperature range of 490-885°C. At these stages, the highest conversions occurred, with activation energy of 2036 kJ/mol and 962.3 kJ/mol, respectively. Similarly for org-MSW samples, the initial low conversion pyrolysis started between 100°C to 203°C, where only 3.82% of the initial weight was converted. The conversion rate intensified above 203°C and then reduced at around 778°C, with this region also divided into two stages: the first between 203°C to 369°C; and the second in the range between 369°C to 778°C, with activation energies of 1116.8 kJ/mol and 635.93 kJ/mol, respectively. Above 778°C, the conversion rate reduced drastically, while its activation energy reached 5284 kJ/mol. Pyrolysis of 50% org-MSW and 50% HVC blend was divided into four stages. First a low conversion rate was observed at temperatures between 100°C and 192°C with an activation energy of 516 kJ/mol. In the temperature ranges of 192°C to 319°C and 319°C to 781°C, the activation energies were 1241 and 582 kJ/mol, respectively. It is evident that HVC and org-MSW blending reduces the activation energies in comparison to non-blended HVC samples and the reduced activation energies were below the expected average based on the original components of the blends.

3.4. Properties of org-MSW and HVC char samples

Thermal property measurements of org-MSW and HVC solid char samples produced at 800°C were conducted according to ASTM D3172 – 13 (see Table 7). It can be seen from Table 2 and Table 4 that org-MSW loses a substantial part of its initial weight due to the release of volatiles during pyrolysis. As a result, the calorific value of the char produced from org-MSW decreased from 17.8 to 13.6 MJ/kg after

pyrolysis. However, calorific values of the HVC samples increased from 26.97 MJ/kg to 31.84 MJ/kg (see Table 7). It should also be noted that the fixed carbon of org-MSW has improved notably from 23.4 to 34.4% between non-pyrolyzed and pyrolyzed samples, respectively. However, for HVC samples, this value has changed from 51.3% to 83.1%. As a result, it could be concluded that co-pyrolysis of highly volatile org-MSW supported with HVC feedstock can produce a reasonable quality char product with low volatile matter. Some changes were also noted on elemental composition. Hydrogen content of org-MSW has decreased from 6.1% to 1.6%, while a similar trend was noted in the HVC samples. In addition, the pyrolysis process has also decreased the carbon content from 46% to 42%, while for HVC the carbon content increased notably from 69.7% to 97%.

Table 7. Proximate and ultimate analysis of char produced at 800°C

Proximate analysis (wt.%)	**Org-MSW**	**HVC**	**Ultimate analysis (wt.%)**	**Org-MSW**	**HVC**
Moisture	0.5	1.4	*Carbon*	41.9	96.6
Volatile matter	13.3	11.6	*Hydrogen*	1.6	1.2
Fixed carbon	34.4	83.1	*Nitrogen*	3.6	2.6
Ash	51.8	3.9	*Sulfur*	0.4	0.3
GCV, MJ/kg	13.6	31.8	*Oxygen**	52.6	0

*By difference

3.5. X-ray diffraction analysis of char

Fig. 7 presents the XRD results for org-MSW and HCV samples before the pyrolysis process. It was observed that due to presence of large amounts of amorphous carbon, XRD peaks could not be distinguished for the org-MSW sample. However,

the HVC sample shows peaks which are probably associated with crystalline carbon contents.

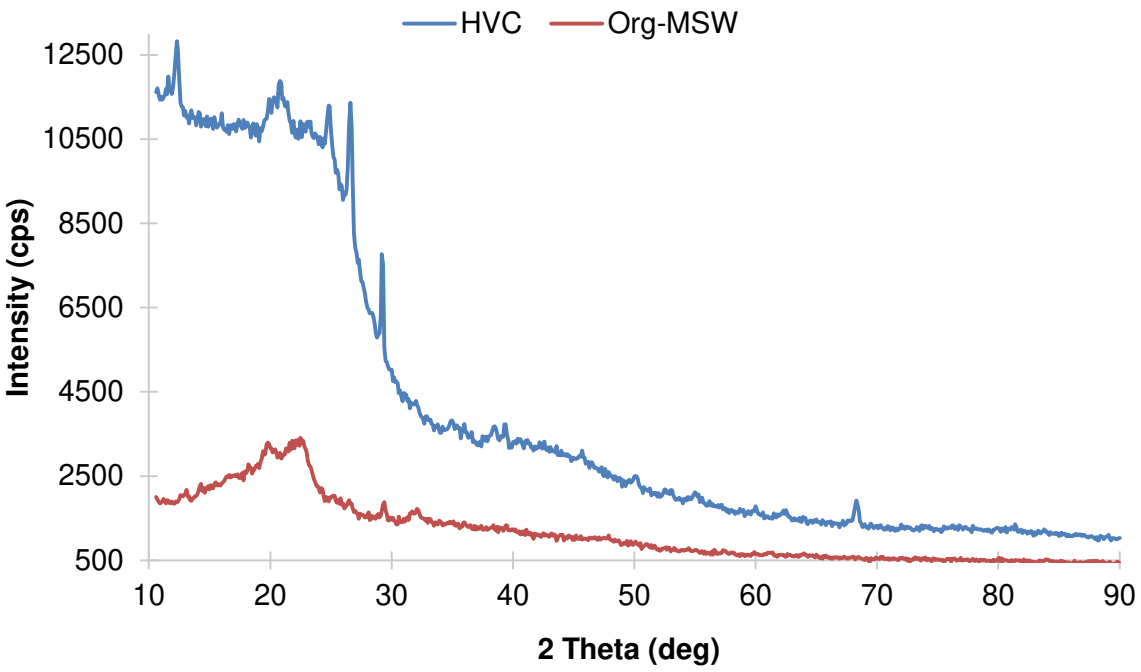

Fig. 7. X-ray diffraction curves for HVC and org-MSW samples before pyrolysis

Fig. 8 (a) gives the XRD curves for HVC, org-MSW and their 50/50 blend from the pyrolysis conducted at 800°C. The XRD patterns of char produced from an org-MSW were comparable with those obtained by Septien et al. [45]. No evidence of crystalline carbon can be found from Fig. 8 (a), suggesting that the char carbon is primarily amorphous. It can also be noted that the blended char samples have more calcite than pure org-MSW or HVC samples. The reason might be the interaction of non-crystalline inorganic species and formation of calcium-based crystals during the pyrolysis of the mixture [46]. Previously, Septien et al. [45] analyzed by XRD char samples of wood particles with 1 mm size that were pyrolyzed at 1000°C and showed that there were no crystalline structures present in the samples. However, analysis of char samples treated at 1400°C showed XRD patterns associated with calcite and vaterite (which may suggest some carbonation during cooling), periclase

MgO and manganese silicate, $MnSiO_3$ [46]. In addition, Lu et al. [47] showed the XRD patterns of graphite and hexagonal ring structures for coal chars produced at a pyrolysis temperature of 1200°C. Similar XRD patterns were determined for the HVC char samples tested in this work.

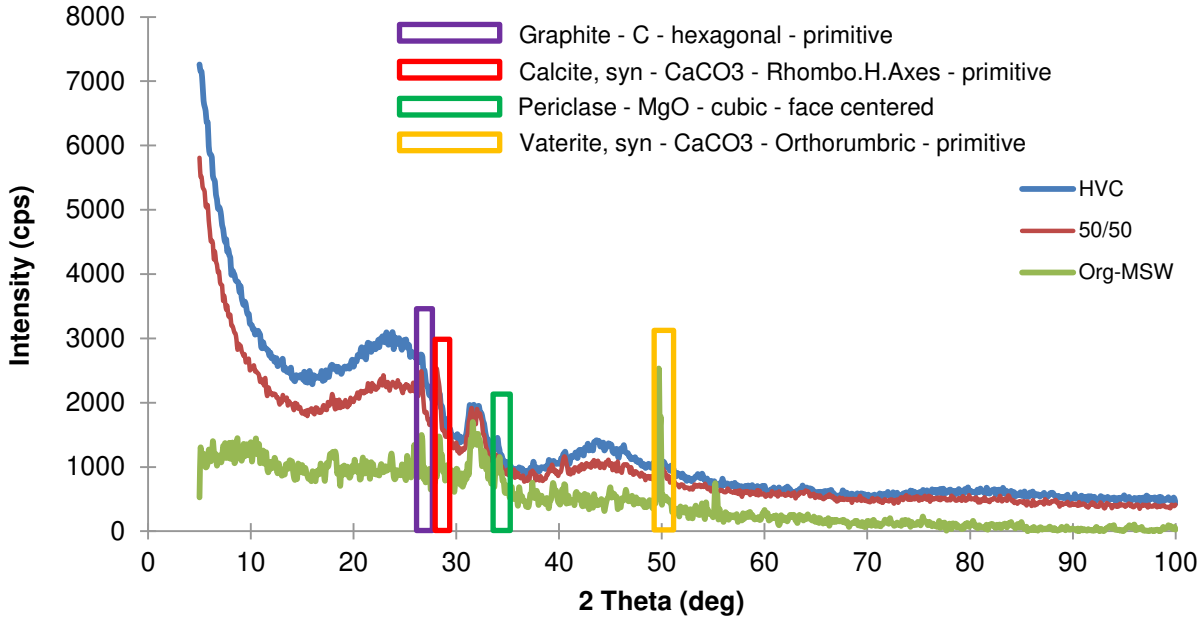

Fig. 8. (a) X-ray diffraction curves for char samples after pyrolysis at 800°C

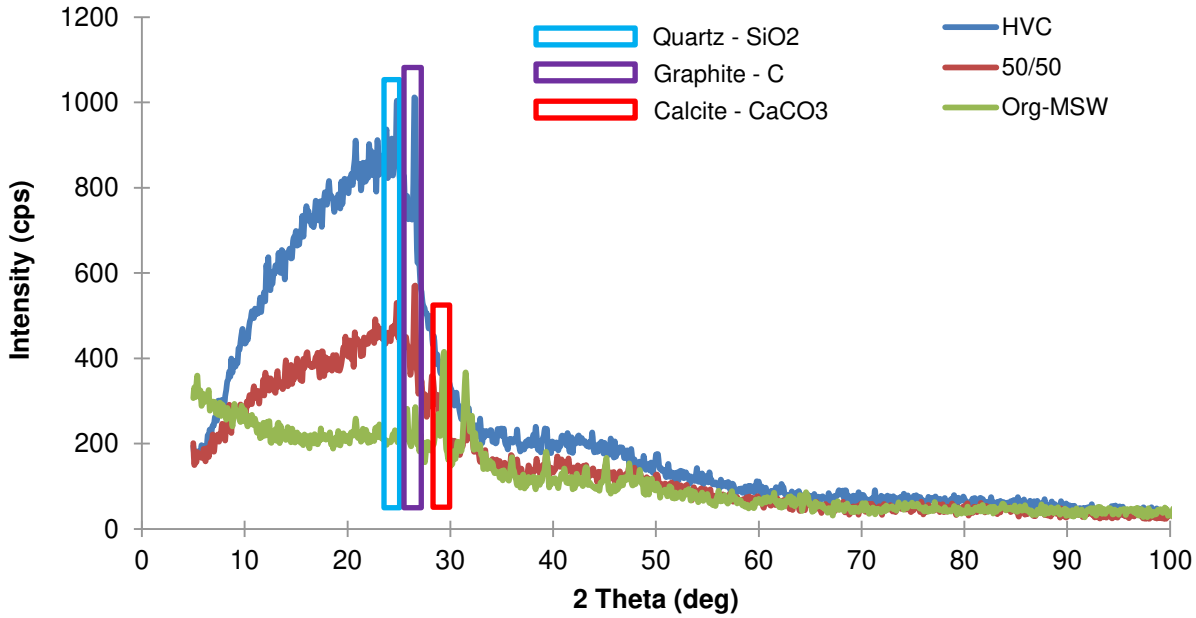

Fig. 8. (b) X-ray diffraction curves for char samples after pyrolysis at 500°C

Fig. 8 (b) shows the XRD patterns for char samples, after low temperature pyrolysis at 500°C, for HVC, org-MSW and their 50/50 blend. Only a few peaks were noted which might be due to the presence of calcite, graphite and quartz in the char samples produced at 500°C.

4. Conclusions

Due to the growing demand for energy, the production of char feedstocks from various waste sources can play a key role towards green energy and circular economy initiatives. In this regard, co-pyrolysis of solid waste fuels such as org-MSW blended with coals can be a reasonable solution to produce valuable biochar feedstocks and other by-products such as syngas and liquids for further processes to support the circular bio-economy initiatives. The results of this work are applicable to most developing countries with high organic waste in the MSW stream, although it is evident that high volatile coal and org-MSW blend pyrolysis is complex due to the heterogeneity of feedstocks. It was observed that an increase in pyrolysis temperature increased the gas yield and decreased the char content for both org-MSW and HVC samples. In addition, it was noted that low-temperature pyrolysis was favored for org-MSW rather than HVC samples. As a result, less volatile matter was released from the char, thus ensuring higher calorific values.

The fixed bed pyrolysis tests at 800°C have resulted in char fractions of 39.2% for org-MSW and 61.8% for HVC (see Table 4). In TGA tests, the residual char weights of similar samples were 28.27% for org-MSW and 60.8% for HVC at 800°C. Further release of volatiles was not observed for HVC samples when increasing the temperature to 900°C. Conversely, a notable change on weight loss was seen with org-MSW samples, when the pyrolysis temperature was increased from 800°C to 900°C in TGA. This probably occurred due to further volatilization of the org-MSW

fraction. In addition, the carbon content of org-MSW char samples has improved from 46% to 49% after pyrolysis.

The temperatures for the most rapid org-MSW and HVC decomposition were found at 306 and 459°C, respectively. It was also observed that major decomposition of org-MSW samples takes place over two temperature windows, the first being from 203°C to 369°C with activation energy of 1117 kJ/mol, and the second occurring between 369°C to 778°C with the highest activation energy of 5284 kJ/mol. In the blended tests of org-MSW and HVC with weight ratio of 50/50%, the highest decomposition occurred in the temperature range of 781-890°C with activation energy of 5106 kJ/mol.

Acknowledgement

The authors would like to thank Nazarbayev University (NU) for funding this work [Project number: 284-2019/012-2019 entitled: *"Development of MSW combustion and incineration technology for Astana (Kazakhstan) and investigation of MSW blending effects on reactivity of coals in CFB combustion and gasification process"*].

References

[1] Hoornweg D, Bhada-Tata P. What a Waste: A Global Review of Solid Waste Management. Urban development series; knowledge papers no. 15.World Bank, Washington, DC. © World Bank. https://openknowledge.worldbank.org/handle/10986/17388. License: CC BY 3.0 IGO. [accessed 20 July 2019].

[2] Indrawan N, Thapa S, Bhoi PR, Huhnke RL, Kumar A. Electricity power generation from co-gasification of municipal solid wastes and biomass: Generation

and emission performance. Energy 2018;162:764-775. https://doi.org/10.1016/j.energy.2018.07.169.

[3] Silpa K, Yao L, Perinaz BT, Woerden FV. What a Waste 2.0 : A Global Snapshot of Solid Waste Management to 2050. Urban Development; Washington, DC: © World Bank. Available at: https://openknowledge.worldbank.org/handle/10986/30317. License: CC BY 3.0 IGO; 2008 [accessed 22 March 2019].

[4] Directive 2008/98/EC of the European Parliament and of the Council on Waste and Repealing Certain Directives – Annex II, 19 November 2008.

[5] Lombardi L, Carnevale E, Corti A. A review of technologies and performances of thermal treatment systems for energy recovery from waste. Waste Manage 2015; 37: 26–44. https://doi.org/10.1016/j.wasman.2014.11.010.

[6] Zhang J, Kan X, Shen Y, Loh K-C, Wang C-H, Dai Y, Tong YW. A hybrid biological and thermal waste-to-energy system with heat energy recovery and utilization for solid organic waste treatment. Energy 2018;152:214-222. https://doi.org/10.1016/j.energy.2018.03.143.

[7] Porteous A. Why energy from waste incineration is an essential component of environmentally responsible waste management. Waste Manage 2005;25: 451-459. https://doi.org/10.1016/j.wasman.2005.02.008.

[8] Malinauskaite J, Jouhara H, Czajczyska D, Stanchev, P, Katsou E, Rostkowski P, Thorne RJ, Colon J, Ponsa S, Al-Mansour F, Anguilano L, Krzyzynska R, Lopez IC, Vlasopoulos A, Spencer N. Municipal solid waste management and waste-to-energy in the context of a circular economy and energy

recycling in Europe. Energy 2017;141:2013-2044. https://doi.org/10.1016/j.energy.2017.11.128.

[9] Rudra S, Tesfagaber YK. Future district heating plant integrated with municipal solid waste (MSW) gasification for hydrogen production. Energy 2019;180:881-892. https://doi.org/10.1016/j.energy.2019.05.125.

[10] Sipra AT, Gao N, Sarwar H. Municipal solid waste (MSW) pyrolysis for bio-fuel production: A review of effects of MSW components and catalysts. Fuel Process Tech 2018;175:131-147. https://doi.org/10.1016/j.fuproc.2018.02.012.

[11] Malkow T. Novel and innovative pyrolysis and gasification technologies for energy efficiency and environmentally sound MSW disposal. Waste Manage 2004;24:53-79. https://doi.org/10.1016/S0956-053X(03)00038-2.

[12] Chen D, Yin L, Wang H, He P. Pyrolysis technologies for municipal solid waste: A review. Waste Manage 2014;34:2466-2486. https://doi.org/10.1016/j.wasman.2014.08.004.

[13] Arena U. Process and technological aspects of municipal solid waste gasification. A review. Waste Manage 2012;32:625-639. https://doi.org/10.1016/j.wasman.2011.09.025.

[14] Consonni S, Viganó F. Waste gasification vs. conventional Waste-To-Energy: A comparative evaluation of two commercial technologies. Waste Manage 2012;32:653-666. https://doi.org/10.1016/j.wasman.2011.12.019.

[15] Chhabra V, Shastri Y, Bhattacharya S. Kinetics of Pyrolysis of Mixed Municipal Solid Waste-A Review, Procedia Environ Sci 2016;35:513–527. https://doi.org/10.1016/j.proenv.2016.07.036.

[16] Yun YM, Seo MW, Ra HW, Koo GH, Oh JS, Yoon SJ, Kim YK, Lee JG, Kim JH. Pyrolysis characteristics of glass fiber-reinforced plastic (GFRP) under isothermal conditions. J Anal Appl Pyrolysis 2015;114:40–46. https://doi.org/10.1016/j.jaap.2015.04.013.

[17] Singh S, Wu C, Williams PT. Pyrolysis of waste materials using TGA-MS and TGA-FTIR as complementary characterisation techniques. J Anal Appl Pyrolysis 2012;94:99–107. https://doi.org/10.1016/j.jaap.2011.11.011.

[18] Fermoso J, Arias B, Plaza MG, Pevida C, Rubiera F, Pis JJ, García-Peña F, Casero P. High-pressure co-gasification of coal with biomass and petroleum coke, Fuel Process Technol 2009;90:926–932. https://doi.org/10.1016/j.fuproc.2009.02.006.

[19] Masnadi MS, Habibi R, Kopyscinski J, Hill JM, Bi X, Lim CJ, Ellis N, Grace JR. Fuel characterization and co-pyrolysis kinetics of biomass and fossil fuels. Fuel 2014;117:1204–1214. https://doi.org/10.1016/j.fuel.2013.02.006.

[20] Zhou L, Luo T, Huang Q. Co-pyrolysis characteristics and kinetics of coal and plastic blends. Energy Convers Manag 2009;50:705–710. https://doi.org/10.1016/j.enconman.2008.10.007.

[21] Cai J, Wang Y, Zhou L, Huang Q. Thermogravimetric analysis and kinetics of coal/plastic blends during co-pyrolysis in nitrogen atmosphere. Fuel Process Technol 2008;89:21–27. https://doi.org/10.1016/j.fuproc.2007.06.006.

[22] Ren Q, Zhao C, Wu X, Liang C, Chen X, Shen J, Tang G, Wang Z. TG-FTIR study on co-pyrolysis of municipal solid waste with biomass. Bioresour Technol 2009;100:4054–4057. https://doi.org/10.1016/j.biortech.2009.03.038.

[23] Havelcová M, Bičáková O, Sýkorová I, Weishauptová Z, Melegy A. Characterization of products from pyrolysis of coal with the addition of polyethylene terephthalate. Fuel Process Technol 2016;154:123–131. https://doi.org/10.1016/j.fuproc.2016.08.022.

[24] Bičáková O, Straka P. Co-pyrolysis of waste tire/coal mixtures for smokeless fuel, maltenes and hydrogen-rich gas production. Energy Convers Manag 2016;116:203–213. https://doi.org/10.1016/j.enconman.2016.02.069.

[25] Guo F, Li X, Wang Y, Liu Y, Li T, Guo C. Characterization of Zhundong lignite and biomass co-pyrolysis in a thermogravimetric analyzer and a fixed bed reactor. Energy 2017;141:2154–2163. https://doi.org/10.1016/j.energy.2017.11.141.

[26] Cordero T, Rodríguez-Mirasol J, Pastrana J, Rodríguez JJ. Improved solid fuels from co-pyrolysis of a high-sulphur content coal and different lignocellulosic wastes. Fuel 2004;83:1585–1590. https://doi.org/10.1016/j.fuel.2004.02.013.

[27] Fang S, Yu Z, Lin Y, Hu S, Liao Y, Ma X. Thermogravimetric analysis of the co-pyrolysis of paper sludge and municipal solid waste. Energy Convers Manag 2015;101:626-631. https://doi.org/10.1016/j.enconman.2015.06.026.

[28] Miranda M, Cabrita I, Pinto F, Gulyurtlu I. Mixtures of rubber tyre and plastic wastes pyrolysis: A kinetic study. Energy 2013;58:270-282. http://dx.doi.org/10.1016/j.energy.2013.06.033.

[29] Tokmurzin D, Aiymbetov B, Abylkhani B, Yagofarova A, Sarbassov Y, Inglezakis V, Venetis C, Poulopoulos SG. Fixed-bed gasification and pyrolysis of organic fraction of MSW blended with coal samples. Chem Eng Trans 2019;7:163–168. https://doi.org/10.3303/CET1972028.

[30] ASTM D3172 – 13. Standard Practice for Proximate Analysis of Coal and Coke. ASTM International, West Conshohocken, PA.

[31] ASTM E870-82 (2019). Standard Test Methods for Analysis of Wood Fuels which were performed in a muffle furnace. ASTM International, West Conshohocken, PA.

[32] ASTM D5373 – 16 Standard Test Methods for Determination of Carbon, Hydrogen and Nitrogen in Analysis Samples of Coal, and Carbon in Analysis Samples of Coal and Coke. ASTM International, West Conshohocken, PA.

[33] ASTM Standard E790-08, 2004. Standard Test Method for Residual Moisture in a Refuse-Derived Fuel Analysis Sample. ASTM International, West Conshohocken,
PA.

[34] ASTM Standard E830-87, 2004. Standard Test Method for Ash in the Analysis Sample of Refuse-Derived Fuel. ASTM International, West Conshohocken, PA.

[35] ASTM Standard E897-88, 2004. Standard Test Method for Volatile Matter in the Analysis Sample of Refuse-Derived Fuel. ASTM International, West Conshohocken, PA.

[36] Gao Z, Li N, Yin S, Yi W. Pyrolysis behavior of cellulose in a fixed bed reactor: Residue evolution and effects of parameters on products distribution and bio-oil composition. Energy 2019;175:1067–1074. https://doi.org/10.1016/j.energy.2019.03.094.

[37] Waheed QMK, Nahil MA, Williams PT, Pyrolysis of waste biomass: investigation of fast pyrolysis and slow pyrolysis process conditions on product yield and gas composition. J Energy Inst 2013;86:233–241. https://doi:10.1179/1743967113Z.00000000067.

[38] Arni SA. Comparison of slow and fast pyrolysis for converting biomass into fuel. Renew Energy 2018;124:197–201. https://doi.org/10.1016/j.renene.2017.04.060.

[39] Bridgwater AV, Carson P, Coulson M. A comparison of fast and slow pyrolysis liquids from mallee. Int J Glob Energy Issues 2007;27:204-216. https://doi:10.1504/IJGEI.2007.013655.

[40] Zhou H, Long Y, Meng A, Li Q, Zhang Y. Thermogravimetric characteristics of typical municipal solid waste fractions during co-pyrolysis. Waste Manage 2015;38:194–200. https://doi.org/10.1016/j.wasman.2014.09.027.

[41] Ferrara F, Orsini A, Plaisant A, Pettinau A. Pyrolysis of coal, biomass and their blends: Performance assessment by thermogravimetric analysis. Bioresour Technol 2014;171:433–441. https://doi.org/10.1016/j.biortech.2014.08.104.

[42] Liu Q, Hu H, Zhou Q, Zhu S, Chen G. Effect of inorganic matter on reactivity and kinetics of coal pyrolysis. Fuel 2004;83:713–718. https://doi.org/10.1016/j.fuel.2003.08.017.

[43] Jiang L, Yuan X, Li H, Xiao Z, Liang J, Wang H, Wu Z, Chen X, Zeng G. Pyrolysis and combustion kinetics of sludge–camphor pellet thermal decomposition using thermogravimetric analysis. Energy Convers Manage 2015;106:282–289. https://doi.org/10.1016/j.enconman.2015.09.046.

[44] Melendi-Espina S, Alvarez R, Diez MA, Casal MD, Coal and plastic waste co-pyrolysis by thermal analysis–mass spectrometry. Fuel Process Technol 2015;137:351-358. https://doi.org/10.1016/j.fuproc.2015.03.024.

[45] Septien S, Valin S, Peyrot M, Dupont C, Salvador S. Characterization of char and soot from millimetric wood particles pyrolysis in a drop tube reactor between 800°C and 1400°C. Fuel 2014;121:216–224. https://doi.org/10.1016/j.fuel.2013.12.026.

[46] Ellis N, Masnadi MS, Roberts DG, Kochanek MA, Ilyushechkin AY. Mineral matter interactions during co-pyrolysis of coal and biomass and their impact on intrinsic char co-gasification reactivity. Chem Eng J 2015;279:402–408. https://doi.org/10.1016/j.cej.2015.05.057.

[47] Lu L, Sahajwalla V, Harris D. Characteristics of Chars Prepared from Various Pulverized Coals at Different Temperatures Using Drop-Tube Furnace. Energy and Fuels 2000;14:869–876. https://doi.org/10.1021/ef990236s.

Characterization of solid char produced from pyrolysis of the organic fraction of municipal solid waste, high volatile coal and their blends

Tokmurzin, Diyar

2019-11-22

Tokmurzin D, Kuspangaliyeva B, Aimbetov B, et al., (2020) Characterization of solid char produced from pyrolysis of the organic fraction of municipal solid waste, high volatile coal and their blends. Energy, Volume 191, January 2020, Article number 116562

https://doi.org/10.1016/j.energy.2019.116562